Analysis of micro-Doppler signatures of moving vehicles by using empirical mode decomposition

Yanbing Li*, Lan Du, Hongwei Liu

National Lab of Radar Signal Processing, Xidian University, Xi'an, China
*e-mail: xidianlyb@163.com

Abstract

This paper utilizes empirical mode decomposition to analyze the micro-motion of moving vehicles. Due to the adaptive function of empirical mode decomposition (EMD), different micro-motion of moving vehicles can be extracted by this decomposition technique. The analysis results based on simulated data and measured data show that special structures of different vehicles can be well depicted by EMD.

Keywords: micro-Doppler, empirical mode decomposition, moving vehicles.

1. Introduction

When a moving target is illuminated by radar, the carrier frequency of its returned signal will be shifted. The value of the frequency shift is called Doppler frequency and determined by the wavelength and the radial velocity of the moving target. If the target has non-rigid-body motion, these non-rigid-body structures may induce additional Doppler modulation on the returned signal, which is called micro-Doppler effect [1]. Since the notion of micro-Doppler was introduced in radar [2], [3], lots of researches based on micro-Doppler effect have been presented [4]-[7], which demonstrate micro-Doppler frequencies accord with target micro-motion and the corresponding micro-Doppler features can be utilized to depict the micro-motion structures of the targets.

For moving vehicles, the micro-motion of wheel is rotation, while the micro-motions of track are more complex which include not only rotation but also translation with fixed ratios relative to the bulk motion. For example, the translation of upper track has the velocity which is always twice as large as the bulk velocity of main body. In addition, the micro-Doppler frequency of upper track is not always observed by radar in practice because of shelter. In this case, an analysis method, namely empirical mode decomposition (EMD) [8] which can elaborately describe the special characteristic of the returned radar signal of moving vehicles, is needed. Cai et al. [9] presented that EMD could separate the micro-motion from the bulk-motion of the target body. Based on their work, this paper shows that EMD can depict the returned signal of special structure of vehicles and detect whether the micro-motion of the upper track is observed by radar.

The rest of this paper is organized as follows. In Section 2, we establish micro-motion model for vehicles. Section 3 reviews the basic principles of EMD and Section 4 applies EMD to the simulated data and measured data of vehicles and presents the analysis of decomposition results. The conclusion is given in Section 5.

2. Micro-Motion Models of wheel and track

When a target moves along the radar line of sight (LOS), the Doppler frequency of its returned signal is:

$$f_d = \frac{2v}{\lambda} \tag{1}$$

where λ is wavelength and v is radial bulk velocity. In order to observe the micro-motion more specifically, λ should be small, i.e., the radar needs to operate in high frequency band. In this case, the Radar Cross Section (RCS) of target can be approximately described by scattering center model [10].

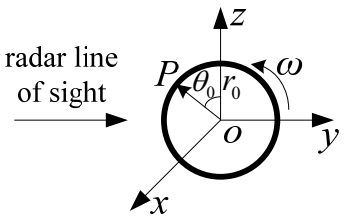

Fig.1. Micro-motion of wheel

In the following discussions of this section, we have the assumption that the radial bulk velocity of vehicle is v, which has been compensated in the analysis of micro-motion structures of vehicles. For a moving wheel as in Fig. 1, it lies in the yoz plane. Assume that there are K scattering points distributed evenly on the wheel edge and the k th scattering point has an initial angle:

$$\theta_k = \theta_0 + 2\pi(k-1)/K \tag{2}$$

with $k = 1, 2, ..., K$ and θ_0 denotes the initial angle of the first scattering point. The returned micro-motion signal of the wheel is represented as [4]:

$$s(t) = \sum_{k=1}^{K} \frac{\xi_k}{\omega} \sum_{n=-\infty}^{\infty} e^{jn\theta_k} J_n(\beta) e^{jn\omega t} \tag{3}$$

with J_n denoting the n th-order Bessel function of the first kind, $\beta = 4\pi r_0/\lambda$, r_0 is the radius of rotation, ω is angle frequency of rotation, and ξ_k is the scattering coefficient of the k th scattering point.

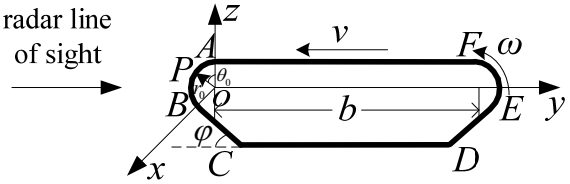

Fig.2. Micro-motion of track

978-1-4244-8443-0/11/$26.00 ©2011 IEEE

For a moving track as in Fig. 2. The returned micro-motion signal is equal to the sum of returned signals generated by parts AB, BC, CD, DE, EF and FA. The micro-motions of part AB and EF are rotation, and the returned signal of EF is added a phase relative to that of AB, which is caused by the length of track denoted by b. The micro-motions of part BC, CD, DE and FA are translation. Based on the assumption that the bulk velocity is v, the rotation angular velocities of part AB and EF with respect to the body of tracked vehicle are $\omega = v / r_0$, and the velocity of part BC, CD, DE and FA with respect to the body are $-v\cos\varphi$, $-v$, $-v\cos\varphi$ and v, respectively. Consequently, the returned micro-motion signal of the track is:

$$\begin{aligned} s(t) &= s_{AB}(t) + s_{BC}(t) + s_{CD}(t) + s_{DE}(t) + s_{EF}(t) + s_{FA}(t) \\ &= \sum_{k=1}^{K_{\mathrm{i}}} \frac{\xi_k}{\omega} \sum_{n=-\infty}^{\infty} e^{jn\theta_k^{\mathrm{i}}} J_n(\beta) e^{jn\omega t} + \\ &\quad \sum_{k=1}^{K_{\mathrm{ii}}} \xi_k \exp[-j\frac{4\pi}{\lambda}(y_k^{\mathrm{ii}} + vt\cos\varphi)] + \\ &\quad \sum_{k=1}^{K_{\mathrm{iii}}} \xi_k \exp[-j\frac{4\pi}{\lambda}(y_k^{\mathrm{iii}} + vt)] + \\ &\quad \sum_{k=1}^{K_{\mathrm{iv}}} \xi_k \exp[-j\frac{4\pi}{\lambda}(y_k^{\mathrm{iv}} + vt\cos\varphi)] + \\ &\quad e^{j\frac{4\pi b}{\lambda}} \sum_{k=1}^{K_{\mathrm{v}}} \frac{\xi_k}{\omega} \sum_{n=-\infty}^{\infty} e^{jn\theta_k^{\mathrm{v}}} J_n(\beta) e^{jn\omega t} + \\ &\quad \sum_{k=1}^{K_{\mathrm{vi}}} \xi_k \exp[-j\frac{4\pi}{\lambda}(y_k^{\mathrm{vi}} - vt)] \end{aligned} \tag{4}$$

where K_{i}, K_{ii}, K_{iii}, K_{iv}, K_{v} and K_{vi} denote the scattering point numbers of parts AB, BC, CD, DE, EF and FA, respectively. φ is the oblique angle of the track, θ_k^u with $u = \mathrm{i}, \mathrm{v}$ denotes the initial angle of the k th scattering point from AB or EF respectively and y_k^u with $u = \mathrm{ii}, \mathrm{iii}, \mathrm{iv}, \mathrm{vi}$ denotes the initial location of the k th scattering point from BC, CD, DE or FA, respectively.

3. Empirical Mode Decomposition

Empirical Mode Decomposition (EMD) is an adaptive analysis tool that decomposes a given signal into a number of "basis functions" which are derived directly from the signal. Component decomposed by EMD is known as Intrinsic Mode Function (IMF) [8]. Given a signal $\mathbf{s}$, the first IMF can be obtained in a systematic way, which is referred to as the sifting process:

(i) Let $\tilde{\mathbf{s}} = \mathbf{s}$.

(ii) Identify the local maxima of $\tilde{\mathbf{s}}$, and interpolate between local maxima to construct an upper envelope $\tilde{\mathbf{s}}_{\mathbf{max}}$.

(iii) Identify the local minima of $\tilde{\mathbf{s}}$, and interpolate between local minima to construct an lower envelope $\tilde{\mathbf{s}}_{\mathbf{min}}$.

(iv) Compute the mean values of upper and lower envelopes as $\tilde{\mathbf{s}}_{\mathbf{mean}} = \frac{\tilde{\mathbf{s}}_{\mathbf{max}} + \tilde{\mathbf{s}}_{\mathbf{min}}}{2}$.

(v) Extract the detail from $\tilde{\mathbf{s}}$: $\mathbf{m} = \tilde{\mathbf{s}} - \tilde{\mathbf{s}}_{\mathbf{mean}}$.

(vi) Let $\tilde{\mathbf{s}} = \mathbf{m}$, and repeatedly apply steps (ii)-(v) to $\tilde{\mathbf{s}}$, until $\mathbf{m}$ is an IMF.

Once the first IMF is obtained, we store the residual $\mathbf{q} = \mathbf{s} - \mathbf{m}$ as a new signal, and the next IMF can be obtained by applying the sifting process to the residual $\mathbf{q}$. In the same way, the remaining IMFs can be calculated and EMD ends up with a representation of the form:

$$\mathbf{s} = \sum_{\alpha=1}^{L} \mathbf{m}_\alpha + \mathbf{q}_{\mathbf{L}} \tag{5}$$

where L is the number of IMFs, $\mathbf{m}_\alpha$ denotes the α th IMF component and $\mathbf{q}_{\mathbf{L}}$ is the residual after L iterations.

The original EMD can only be applied to univariate (real-valued) signal, Rilling et al. [11] propose an approach to extend EMD from univariate case to bivariate case in order to deal with some areas using complex-valued signal structures such as sonar and radar.

4. Analysis of Simulated and Measured Data by using EMD

4.1 Analysis of Simulated data with EMD

The simulated data which include one wheeled vehicle and one tracked vehicle are generated according to the micro-motion model proposed in section 2. The parameters of vehicles and radar are given in table 1 and table 2 respectively.

Table 1 the parameter of target

	Radius (m)	oblique angle (rad)	Length (m)
The wheeled	0.2	-	-
The tracked	0.3	π/8	4

Table 2 the parameter of radar

carrier frequency	PRF
10GHz	3000Hz

The Doppler spectra of original signal and decomposition components for each vehicle are shown in fig. 3. When the motion of mainbody is considered, the returned micro-Doppler echo described in (3) or (4) should be added to a phase term which is induced by the bulk velocity namely v, thus the micro-Doppler frequencies will distributes between the frequency bins representing 0 and $2v$. The spectrum of wheeled vehicle as in fig. 3a contained the bulk-Doppler frequency induced by v, and small micro-Doppler frequencies induced by the rotation part distributing between the frequency bins representing 0 and $2v$. For the tracked vehicle as in fig. 3b, besides the bulk-Doppler frequency and small micro-Doppler frequencies distributing between 0 and $2v$ induced by the rotation part AB and EF, there are three obvious frequencies induced by micro-motion parts which have translation relative to the main body. The first one is the frequency induced by the upper track which represents the double of bulk velocity, we refer it as $2v$ -component; the second one locates at the 0 frequency which is induced by the lower track; the third one is close to the second one, and it is induced by the part BC and part DE of track.

The Doppler spectra of the first IMF, the second IMF and the residual for wheeled vehicle are shown in fig. 3c, fig. 3e and fig. 3g respectively. The first IMF contains the most frequencies of original signal including the bulk-Doppler

frequency and most micro-Doppler frequencies, the rest decomposition components contain limited amounts of frequencies whose amplitudes are very weak.

The Doppler spectra of the first IMF, the second IMF and the residual for tracked vehicle are shown in fig. 3d, fig. 3f and fig. 3h respectively. The first IMF captures the $2v$ -component and the second IMF mainly contains the bulk-Doppler frequency, the other micro-Doppler frequencies are contained in the residual. The decomposition results for tracked vehicle indicate that the EMD separates the micro-motion of upper track, main body and lower track. As a result, the micro-motion structure of track can be well depicted.

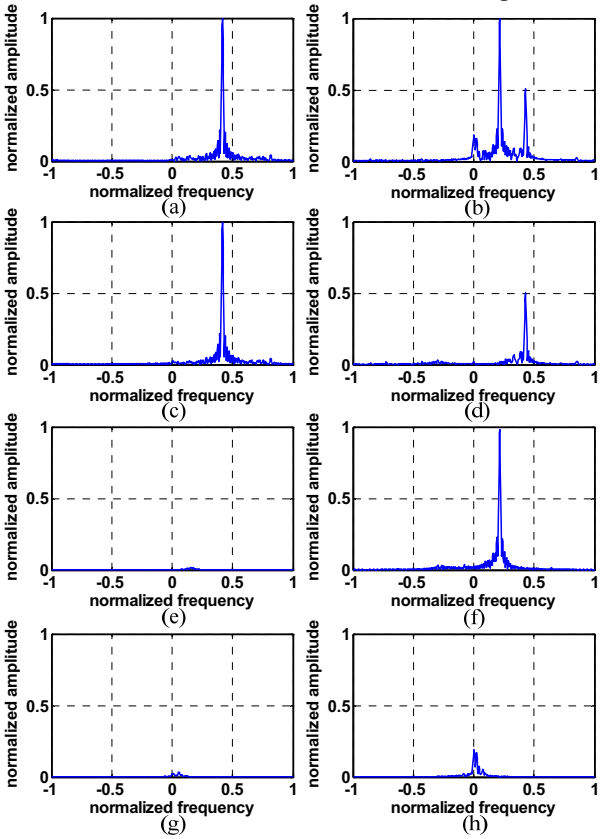

Fig.3. Doppler spectra of original signal and decomposition components for vehicles from simulated data. (a) Original signal of wheeled vehicle. (b) Original signal of tracked vehicle. (c) The first IMF of wheeled vehicle. (d) The first IMF of tracked vehicle. (e) The second IMF of wheeled vehicle. (f) The second IMF of tracked vehicle. (g) The residual of wheeled vehicle. (h) The residual of tracked vehicle.

4.2 Analysis of Measured data with EMD

Measured data are collected from one wheeled vehicle and one tracked vehicle under experimental scenario that the vehicle approaches radar. In the process of data collection, we refer to the number of pulses in a Coherent Processing Interval (CPI) as a frame.

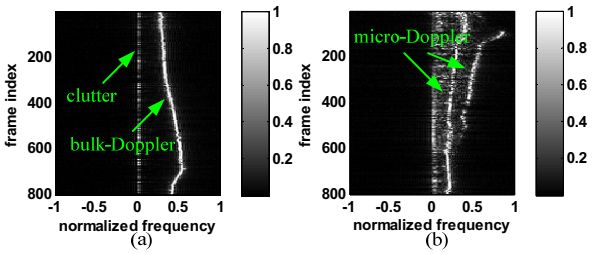

Fig.4. Group Doppler spectra of vehicles. (a) Wheeled vehicle. (b) Tracked vehicle.

Group Doppler spectra of vehicles are illustrated in Fig. 4, where the different shades of gray represent the amplitude of Doppler spectra. For the wheeled vehicle as in Fig. 4a, the entire Doppler spectrum plane is dominated by the bulk-Doppler and clutter, the micro-Doppler frequencies is scarcely observed due to the material of wheel, namely rubber, which hardly scatters the electromagnetic wave in real world scenario. For the tracked vehicle as in Fig. 4b, the remarkable micro-Doppler frequencies can be observed in the Doppler spectrum plane. In addition, it can be seen that $2v$ -components only exist in the Doppler spectra for the frames indexed from 100 to 500, which means the $2v$ -component can not be always observed in practice because of the shelter of upper track.

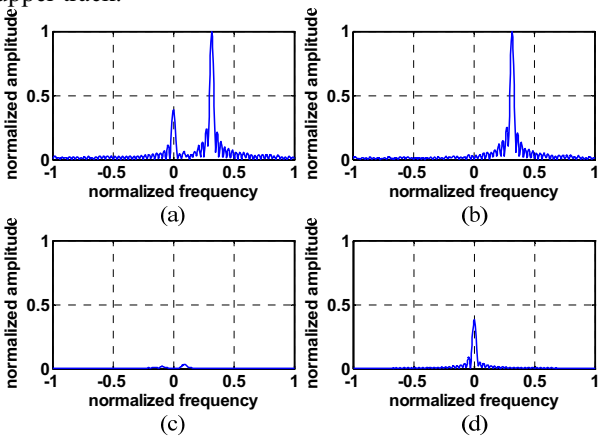

Fig.5. Doppler spectra of original signal and decomposition components for wheeled vehicle from measured data. (a) Original signal. (b) The first IMF. (c) The second IMF. (d) The residual.

The Doppler spectra of original signal and decomposition components for the wheeled vehicle are shown in fig. 5. The spectrum of the wheeled vehicle as in fig. 5a is much like that from simulated data except the ground clutter around 0 frequency. The first IMF contains bulk-Doppler frequency as in fig. 5b while the second IMF contains few frequencies as in fig. 5c. The residual mainly contain the clutter as in fig. 5d. These decomposition results are similar to those from simulated data for wheeled vehicle, and they show that EMD can separate the bulk-Doppler frequency from the clutter for the wheeled vehicle in practice.

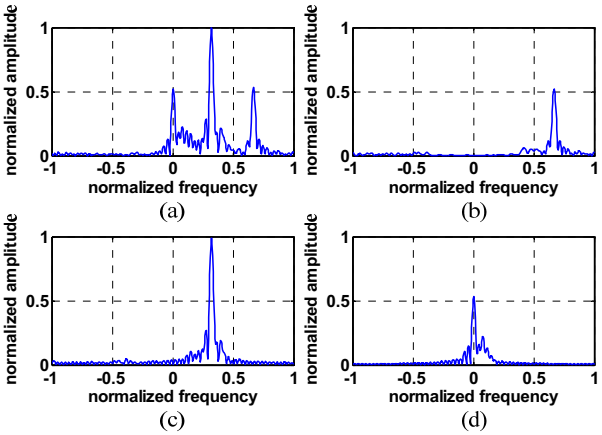

Fig.6. Doppler spectra of original signal and decomposition components for tracked vehicle with 2v-component from measured data. (a) Original signal. (b) The first IMF. (c) The second IMF. (d) The residual.

Because the 2v-component is not always observed by radar, the analysis for tracked vehicle includes two cases: one is that the 2v-component is observed and the other is the 2v-component does not exist.

In the first case as shown in fig. 6a, the decomposition results are similar to those of simulated data, that is to say the 2v-component is contained in the first IMF as in fig. 6b and the bulk-Doppler is contained in the second IMF as in fig.6c, clutter and a few micro-Doppler frequencies are contained in the residual as in fig.6d.

As to the second case as shown in fig. 7a, the first IMF as in fig. 7b contains the bulk-Doppler and the second IMF as in fig. 7c contains the micro-Doppler frequencies, clutter and a few micro-Doppler frequencies are contained in the residual as in fig.7d.

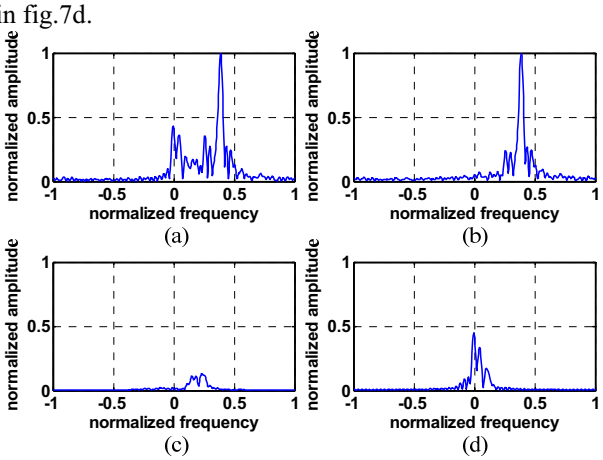

Fig.7. Doppler spectra of original signal and decomposition components for tracked vehicle without 2v-component from measured data. (a) Original signal. (b) The first IMF. (c) The second IMF. (d) The residual.

The decomposition results with and without 2v-component for tracked vehicle indicate that EMD can not only extract the interesting frequencies such as the 2v-component and the bulk-Doppler from clutter in practice but also detect the existence of 2v-component, i.e. if the 2v-component is observed by radar, the first IMF will capture it.

5. Conclusions

For moving vehicles, micro-motion structures of the wheeled vehicle and the tracked vehicle induce different micro-Doppler modulations. As an adaptive analysis technique, EMD can separate the bulk-Doppler, the micro-Doppler and the ground clutter from each other for vehicles. Moreover, for complex structures such as track, EMD can further detect and extract unique micro-Doppler frequency namely 2v-component. Thus the features of moving vehicles can be well expressed from the decomposition results, which is suitable for the further processing.

References

[1] M.S. Zediker, R.R. Rice, J.H. Hollister, Method for extending range and sensitivity of a fiber optic micro-Doppler ladar system and apparatus therefore, U.S. Patent 6,847,817, December 1998.

[2] V.C. Chen, F. Li, S.S. Ho, et al., “Analysis of micro-Doppler signatures”, IEE Proceedings - Radar, Sonar and Navigation, vol. 150, pp. 271-276, 2003.

[3] V.C. Chen, F. Li, S.S. Ho, et al., “Micro-Doppler effect in radar: phenomenon, model, and simulation study”, IEEE Transactions on Aerospace and Electronic System, vol. 42, pp. 2-21, 2006.

[4] T. Thayaparan, S. Abrol, E. Riseborough, et al., “Analysis of radar micro-Doppler signatures from experimental helicopter and human data”, IET Radar, Sonar and Navigation, vol. 1, pp. 289-299, 2007.

[5] V.C. Chen, “Doppler signatures of radar backscattering from objects with micro-motions”, IET Signal Processing, vol. 2, pp. 291-300, 2008.

[6] Y. Kim, H. Ling, “Human activity classification based on micro-Doppler signatures using an artificial neural network”, IEEE Antennas and Propagation Society International Symposium, San Diego, CA, 2008, pp. 1-4.

[7] Y. Kim, H. Ling, “Human activity classification based on micro-Doppler signatures using a support vector machine”, IEEE Transactions on Geoscience and Remote Sensing, vol. 47, pp. 1328-1337, 2009.

[8] N.E. Huang, Z. Shen, S.R. Long, et al., “The empirical mode decomposition and the Hilbert spectrum for nonlinear and non-stationary time series analysis”, Proceedings of the Royal Society of London. Series A: Mathematical, Physical and Engineering Sciences, vol. 454, pp. 903-995, 1998.

[9] C.J. Cai, W.X. Liu, J.S. Fu, et al., “Empirical mode decomposition of micro-Doppler signature”, 2005 IEEE International Radar Conference, May 2005, pp. 895-899.

[10] W.G. Carrara, R.S. Goodman, R.M. Majewski, Spotlight synthetic aperture radar - signal processing algorithms, Norwood, MA: Arthech House, 1995.

[11] G. Rilling, P. Flandrin, P. Goncalves, et al., “Bivariate empirical mode decomposition”, IEEE Signal Processing Letters, vol. 14, pp. 936-939, 2007.